Physical Communication 66 (2024) 102451

Contents lists available at ScienceDirect

Physical Communication

journal homepage: www.elsevier.com/locate/phycom

Full length article

On the performance of OFDM-IM systems in the presence of CFO effects

Mokhtar Besseghier [a,b,*], Samir Ghouali [a], Ahmed Bouzidi Djebbar [b], Ertugrul Basar [c]

[a] University of Mustapha Stambouli Mascara, Algeria
[b] Telecommunications and Digital Signal Processing Laboratory, University of Sidi-Bel-Abbes, Algeria
[c] Communications Research and Innovation Laboratory (CoreLab), Department of Electrical and Electronics Engineering, Koc University, Turkey

ARTICLE INFO

Keywords:
OFDM-IM
CFO
SNR
BER
ICI

ABSTRACT

This study presents a comprehensive analysis of the performance degradation effects of carrier frequency offset (CFO) on orthogonal frequency division multiplexing with index modulation (OFDM-IM) systems operating over frequency-selective multipath fading channels. CFO is an impairing factor that degrades the signal-to-noise ratio (SNR) through signal attenuation and inter-carrier interference (ICI). We derive a closed-form expression to quantify the SNR degradation under CFO for OFDM-IM systems. Additionally, we formulate a very tight upper bound for the bit error rate (BER), accounting for index modulation errors, CFO distortion, and multipath fading.

The presented analytical formulations capture the unique characteristics of OFDM-IM systems and facilitate precise performance evaluation. The findings yield valuable insights into mitigating CFO-induced BER degradation through appropriate system parameter selection and CFO compensation techniques. Moreover, this investigation makes significant contributions towards designing reliable OFDM-IM communication links resilient to the combined effects of index modulation, frequency offsets, and dispersive channel conditions.

1. Introduction

Orthogonal frequency division multiplexing (OFDM) has emerged as the prominent modulation technique for modern broadband wireless communications due to its inherent resilience to delay spread and inter-symbol interference [1]. To further enhance spectral efficiency, the concept of index modulation (IM) has gained significant traction, where additional information bits are conveyed by selectively activating a subset of subcarriers [2–6]. IM has evolved into various enhanced schemes, such as multiple-mode OFDM-IM [7], composite OFDM-IM [8], and joint-mapping OFDM [9], offering improved performance and flexibility for diverse applications. This unique modulation approach has found applications in emerging domains such as 6G communications [10], private 5G networks [11], and the green Internet of Things (IoT) [12]. While OFDM-IM offers promising gains in spectral efficiency, its practical implementation is susceptible to the deleterious effects of carrier frequency offsets (CFOs). CFO, which is inevitable in real-world scenarios due to oscillator drifts, Doppler shifts, and synchronization errors, can disrupt the critical subcarrier orthogonality and attenuate the desired signal [13]. These impairments lead to inter-carrier interference (ICI) and signal-to-noise ratio (SNR) degradation, ultimately compromising overall system performance. Although the impact of CFOs on classical OFDM systems has been extensively studied [14–16], the unique characteristics of OFDM-IM necessitate dedicated analysis to characterize the specific consequences on its performance metrics. Several works have investigated certain aspects of CFO effects on OFDM-IM, such as error probability analysis [17–19], CFO resistance [20], and CFO estimation techniques [13,21]. However, these works primarily focus on isolated aspects and lack a comprehensive, unified framework that captures the interplay between different CFO-induced impairments, such as SNR degradation, index detection errors, and data demodulation errors. Specifically, studies on error probability analysis [17–19] derived expressions for the bit error rate (BER) or pairwise error probabilities under CFO but did not provide insights into the underlying phenomena causing performance degradation. Works on CFO estimation [13,21] addressed the important aspect of CFO compensation but did not analyze the overall performance impact of residual CFOs. The study in [20] investigated waveform designs for enhancing CFO resistance, but did not offer a general analytical treatment for OFDM-IM systems. To address this gap, this paper presents a comprehensive analytical framework to quantify the performance degradation effects caused by CFOs on OFDM-IM systems operating over frequency-selective multipath fading channels. The primary objectives are:

1. To derive closed-form expression that quantify the CFO-induced SNR degradation in OFDM-IM systems, accounting for signal attenuation and ICI.

* Corresponding author at: University of Mustapha Stambouli Mascara, Algeria.
E-mail address: m.besseghier@univ-mascara.dz (M. Besseghier).

https://doi.org/10.1016/j.phycom.2024.102451
Received 4 May 2024; Received in revised form 28 June 2024; Accepted 16 July 2024
Available online 20 July 2024

2. To develop a tight upper bound for the BER performance under CFO impairment, considering the joint impacts of IM errors, CFO distortion, and multipath fading effects.
3. To validate the derived analytical expressions through extensive Monte Carlo simulations across various system configurations and CFO levels.
4. To provide valuable insights into mitigating CFO-induced performance degradation through appropriate system parameter selection and CFO compensation techniques.

In line with the main motivation of our paper, its key contributions are given as follows:

1. New closed-form expression to quantify the SNR penalty caused by CFOs in OFDM-IM systems.
2. Tight upper bound expression for the BER under CFO impairment, accounting for the reliability of index detection based on index bit errors (IBER) and the accuracy of data symbol demodulation based on symbol bit errors (SBER).
3. Comprehensive analysis of the interplay between CFO, index detection reliability, and data demodulation accuracy in OFDM-IM systems.
4. Rigorous validation of the analytical models through Monte Carlo simulations and insightful discussions on practical implications and potential mitigation techniques.

Overall, this investigation offers a comprehensive analysis of tackling the specific issues induced by CFO impairment in OFDM-IM transceivers, to facilitate their future field deployment.

The remainder of this paper is organized as follows: Section 2 the OFDM-IM system model is presented. Section 3 analyzes the detrimental impact of CFO on OFDM-IM signals, deriving closed-form expression to quantify the resulting SNR degradation. Section 4 provides a tight upper bound for the BER under CFO, accounting for IM errors, CFO distortion, and multipath fading effects. The validation of the derived analytical expressions is carried out in Section 5 through extensive Monte Carlo simulations across various system configurations. Finally, Section 6 concludes the paper by summarizing the key findings and outlining potential future research directions in this domain.

1.1. Notation

Throughout this paper, upper (lower) boldface letters indicate matrices (column vectors). $C(N_{sb}, K_{sb})$ denotes the binomial coefficient for N_{sb} choose K_{sb}. $\lfloor . \rfloor$ is the floor function, and $|.|$ stands for the absolute value.

2. System model

The considered OFDM-IM scheme utilizes IM in conjunction with M-ary symbol modulation across a total of N available subcarriers [22]. These N subcarriers are evenly partitioned into G disjoint subblocks, with each subblock g consisting of a subgroup of $N_{sb} = \frac{N}{G}$ adjacent subcarriers. Within each subblock g, a set of p incoming bits undergoes a two-step bit-to-symbol mapping process:

1. Index Modulation: The first $p_1 = \lfloor \log_2 C(N_{sb}, K_{sb}) \rfloor$ bits determine the indices of K_{sb} activated subcarriers out of N_{sb} available per subblock. This is facilitated by a look-up table that maps the p_1 bits to one of 2^{p_1} index combinations $\boldsymbol{\alpha} = \{\alpha_0, \alpha_1, \ldots, \alpha_{K_{sb}-1}\}$, with each index $\alpha_k \in \{0, 1, \ldots, N_{sb} - 1\}$ [23].
2. Symbol Modulation: The next $p_2 = K_{sb} \log_2 M$ bits are M-ary modulated to constellation symbols $\{S_m(0), \ldots, S_m(K_{sb} - 1)\}$. These symbols are conveyed over the K_{sb} active subcarriers indexed by $\boldsymbol{\alpha}$, while the remaining $(N_{sb} - K_{sb})$ inactive subcarriers are nulled out.

In each OFDM block, the time-domain samples $s_m[n]$, $0 \le n \le N + N_{cp} - 1$, are made by an N-point Inverse Discrete Fourier Transform (IDFT) that takes the IDFT across all the symbols in the subblocks. We can formulate it mathematically as follows

$$s_m[n] = \frac{1}{\sqrt{G}} \sum_{g=0}^{G-1} s_{m,g}[n]. \tag{1}$$

Here, $s_{m,g}[n]$ present the signal originating from the gth sub-block within the mth OFDM block, and is expressed as

$$s_{m,g}[n] = \frac{1}{\sqrt{K}} \sum_{k=0}^{K-1} S_m[Kg + k] e^{j2\pi(Ng+\alpha_k)(n-N_{cp})/N} \tag{2}$$

where N_{cp} denotes the number of inserted cyclic prefix (CP) samples, and $K = GK_{sb}$ represents the total number of active subcarriers in each OFDM block. The transmitted signal $s_m[n]$ passes through a frequency-selective multipath fading channel $h_m[n]$ that exhibits block stationarity with time-invariance over each OFDM block with L taps are independent and identically distributed (iid) with $\mathcal{CN}(0, P_h)$.

At the receiver, the signal gets altered by the carrier frequency offset ξ normalized to subcarrier spacing Δf, undergoes convolution with the channel response $h_m[n]$, and gets impaired by noise as follows

$$y_m[n] = e^{j2\pi\xi(n+m(N+N_{cp}))/N} (h_m[n] * s_m[n]) + b_m[n] \tag{3}$$

where $h_m[n] * s_m[n] = \sum_{i=-\infty}^{\infty} h_m[i] s_m[n-i]$ and $b_m[n]$ is an independent additive white Gaussian noise (AWGN) sample with zero-mean and variance σ_b^2.

3. Effect of CFO

CFO can severely degrade the performance of OFDM systems by attenuating the desired signal and introducing ICI, resulting in reduced SNR. This section quantifies the impact of CFO on the SNR in OFDM-IM systems.

The CFO effect can be modeled as a complex multiplicative distortion on the time-domain received signal, applied uniformly across all subcarriers. As illustrated in (3), this distortion consists of a phase shift in time, parameterized by the frequency offset variable ξ. To simplify the analysis, this time-domain phase shift is encapsulated in a variable $c_m[n]$, which represents the phase rotation seen by the signal sample at time index n:

$$c_m[n] \triangleq \frac{1}{\sqrt{K}} e^{j2\pi\xi(n+m(N+N_{cp}))/N}. \tag{4}$$

The received sample $y_m[n]$ can then be expressed as

$$y_m[n] = \sqrt{K} c_m[n] (h_m[n] * s_m[n]) + b_m[n]. \tag{5}$$

This formulation separates the CFO distortion term $c_m[n]$ from the desired signal component $(h_m[n] * s_m[n])$ and the noise term $b_m[n]$. After removing cyclic prefix (CP) and applying fast Fourier transform (FFT), the received signal in the frequency domain $Y_m[k]$ at the kth subcarrier is formulated as

$$Y_m[k] = C_m[k] * (H_m[k] S_m[k]) + B_m[k]. \tag{6}$$

Here, $C_m[k]$, $H_m[k]$, and $B_m[k]$ denote the frequency-domain representations of the CFO distortion, channel response, and noise terms respectively. $C_m[k]$ can be expressed as

$$\begin{aligned} C_m[k] &= \frac{1}{\sqrt{N}} \sum_{n=0}^{N-1} c_m[n] e^{-j2\pi kn/N} \\ &= \frac{1}{\sqrt{KN}} \left(\sum_{n=0}^{N-1} e^{j2\pi(\xi-k)n/N} \right) e^{j2\pi\xi m(N+N_{cp})/N} \\ &= \frac{1}{\sqrt{KN}} \left(\frac{1 - e^{j2\pi(\xi-k)}}{1 - e^{j2\pi(\xi-k)/N}} \right) e^{j2\pi\xi m(1+\beta)} \\ &= \frac{\sin(\pi(\xi-k))}{\sqrt{KN}\sin(\pi(\xi-k)/N)} e^{j\pi(\xi-k)(1-(1/N))} e^{j2\pi\xi m(1+\beta)} \end{aligned} \tag{7}$$

where $\beta = N_{cp}/N$, while the magnitude $|C_m[k]|$ can be expressed as

$$\begin{aligned} |C_m[k]| &= \left| \frac{1}{\sqrt{N}} \sum_{n=0}^{N-1} c_m[n] e^{-j2\pi nk/N} \right| \\ &\leq \frac{1}{\sqrt{N}} \sum_{n=0}^{N-1} |c_m[n] e^{-j2\pi nk/N}| = \sqrt{\frac{N}{K}}. \end{aligned} \tag{8}$$

In this analysis, the received signal $H_m[k]S_m[k]$ on the kth subcarrier is treated as the desired signal. This desired signal is impacted by the CFO distortion $|C_m[0]|$, and phase-rotated by $e^{j\pi[\xi(1-1/N)+2\xi m(1+\beta)]}$. In addition to attenuating the desired signal, CFO also disrupts the critical subcarrier orthogonality, causing ICI. This ICI acts as an additional noise component, further degrading the SNR, where is characterized by

$$I_m[k] \triangleq \sum_{r=1}^{K-1} C_m[r] H_m[k-r] S_m[k-r]. \tag{9}$$

Along with the ICI, background noise $B_m[k]$ also corrupts the received subcarrier signal. Taken together, the overall interference-plus-noise in the received signal in (6), can be rewritten as

$$Y_m[k] = C_m[0] H_m[k] S_m[k] + I_m[k] + B_m[k]. \tag{10}$$

This alternative expression decomposes the received signal into the attenuated and rotated desired signal, ICI, and noise. Building on this reformulated received signal model in (10), the SNR expression for the kth subcarrier can be derived as follows

$$\rho[k] = \frac{E[|C_m[0] H_m[k] S_m[k]|^2]}{E[|I_m[k] + B_m[k]|^2]}. \tag{11}$$

As the channel $H_m[k]$ is independent of the transmit symbol $S_m[k]$, this numerator can be simplified as

$$E[|C_m[0] H_m[k] S_m[k]|^2] = |C_m[0]|^2 P_h \sigma_S^2. \tag{12}$$

Here, $E[|H_m[k]|^2] = P_h$ represents the average channel power, and $E[|S_m[k]|^2] = \sigma_S^2$ denotes the transmit symbol power. The denominator represents the total power of the interference-plus-noise. As described previously, this consists of both ICI power and background noise power

$$E[|I_m[k] + B_m[k]|^2] = E[|I_m[k]|^2] + E[|B_m[k]|^2]. \tag{13}$$

The ICI power term can be expressed as

$$E[|I_m[k]|^2] = \sum_{r=1}^{K-1} |C_m[r]|^2 P_h \sigma_S^2. \tag{14}$$

Applying Parseval's theorem, (14) can be simplified as

$$\sum_{r=0}^{K-1} |C_m[r]|^2 = \sum_{n=0}^{N-1} |c_m[n]|^2 = \frac{N}{K}. \tag{15}$$

Here, a fundamental property of the DFT is utilized along with the fact that $|c_m[n]| = \frac{1}{\sqrt{K}}$ according to (4). Therefore, the ICI power $E[|I_m[k]|^2]$ can be rewritten as

$$E[|I_m[k]|^2] = \left(\frac{N}{K} - |C_m[0]|^2 \right) P_h \sigma_S^2 \tag{16}$$

with $E[|b_m[k]|^2] = \sigma_b^2$. Using (7), $|C_m[0]|^2$ can be expressed as follows

$$|C_m[0]|^2 = \left(\frac{\sin(\pi\xi)}{\sqrt{NK} \sin(\pi\xi/N)} \right)^2. \tag{17}$$

As $N \gg \xi$, the sine function $\sin(\frac{\pi\xi}{N})$ can be approximated as $\sin(\frac{\pi\xi}{N}) \approx \frac{\pi\xi}{N}$, then

$$|C_m[0]|^2 = \frac{N}{K} \mathrm{sinc}^2(\xi). \tag{18}$$

Here $\mathrm{sinc}(x) = \frac{\sin(\pi x)}{\pi x}$. This ultimately allows formulating the SNR dependence on the normalized carrier frequency offset ξ, as given by

$$\rho(\xi) = \frac{N \mathrm{sinc}^2(\xi) P_h \sigma_S^2}{N \left(1 - \mathrm{sinc}^2(\xi)\right) P_h \sigma_S^2 + K \sigma_b^2}. \tag{19}$$

The derived SNR expression $\rho(\xi)$ explicitly captures the dependence on the normalized carrier frequency offset ξ, allowing the quantification of SNR degradation due to a specific frequency offset ξ, by comparing to the case without impairment ($\xi = 0$):

$$D(\xi) \triangleq \frac{\rho(0)}{\rho(\xi)}. \tag{20}$$

Here, $\rho(0)$ represents of SNR in the case absence of CFO, also known as the initial SNR. Substituting the previously derived expression for $\rho(\xi)$ from (19) into (20), the degradation metric can be expanded as

$$D(\xi) = \frac{N(1 - \mathrm{sinc}^2(\xi)) P_h \sigma_S^2 + K \sigma_b^2}{K \sigma_b^2 \mathrm{sinc}^2(\xi)}. \tag{21}$$

The SNR degradation metric $D(\xi)$ quantifies the severity of degradation due to a specific frequency offset ξ by comparing it to the case without impairment ($\xi = 0$). The closed-form expression for $D(\xi)$ in (21) reveals the interplay between various system parameters, such as the number of subcarriers N, the number of active subcarriers K, the channel power P_h, the transmit symbol power σ_S^2, and the noise variance σ_b^2, in determining the overall SNR degradation under CFO.

4. BER analysis under CFO

In the presence of CFO, the received signal experiences both attenuation and phase rotation, as modeled in the previous section. This causes SNR degradation, quantified by the degradation metric $D(\xi)$. Additionally, CFO leads to a loss of subcarrier orthogonality, resulting in ICI. The ICI effect increases the effective noise variance, further impacting the BER performance. Therefore, we analytically evaluate the BER of the proposed OFDM-IM scheme using the low-complexity greedy detector (GD) detection [24]. Building on the work by Crawford et al. [25], the BER for the proposed scheme can be evaluated by considering the two constituent error events: index bit errors and M-ary data bit errors. The index bit errors emerge from inaccurate detection of the active subcarrier indices, which dictates the modulation pattern. As derived in [26], the IBER depends on the probability of index detection error events, which can be analyzed based on the subcarrier SNR distribution. Additionally, the M-ary data symbol bit error rate results from errors in demodulation once the index pattern is determined. The SBER can be computed from the post-detection SNR and modulation constellation density using classical approximate expressions. Therefore, the overall BER under CFO distortion ξ can be expressed as

$$P_b(\xi) = \frac{p_1 P_1(\xi) + p_2 P_2(\xi)}{p_1 + p_2} \tag{22}$$

where $P_1(\xi)$ is the IBER, $P_2(\xi)$ is the SBER, and p_1, p_2 are the number of bits per index symbol and per M-ary symbol respectively.

This formulation reveals the coupled dependence of the overall BER on both the reliability of index detection and the accuracy of data demodulation. The subsequent analysis focuses on quantifying $P_1(\xi)$ and $P_2(\xi)$ under the impact of CFO.

4.1. Index bit errors under CFO

CFO distortion and interference affects the detection of active subcarrier indices, increasing probability of index errors P_1. Using analysis in [26], P_1 depends on the instantaneous index error probability as function of the distorted and interfered subcarrier SNRs under CFO. Let $P_{I|\alpha}(\xi)$ denote the instantaneous probability that subcarrier α is incorrectly detected as inactive under the CFO distortion ξ. As derived in [25], the instantaneous index error probability can then be upper bounded as

$$P_I(\xi) \leq \sum_{\alpha=1}^{N} \left(\frac{K}{N} \right) P_{I|\alpha}(\xi) \tag{23}$$

where (K/N) represents the a priory probability of subcarrier activation. The instantaneous probability $P_{I|\alpha}(\xi)$ can be provided as follows

$$P_{I|\alpha}(\xi) \leq \sum_{\widetilde{\alpha}=1,\widetilde{\alpha}\neq\alpha}^{N-K} P_{\alpha\to\widetilde{\alpha}}(\xi). \tag{24}$$

Here, $P_{\alpha\to\widetilde{\alpha}}(\xi)$ denotes the probability of the pairwise error event $\alpha \to \widetilde{\alpha}$, where the active subcarrier index α is erroneously detected as an inactive index $\widetilde{\alpha} \neq \alpha$ under CFO distortion ξ. Using the GD detector, this pairwise error probability can be obtained as

$$\sum_{\widetilde{\alpha}=1,\widetilde{\alpha}\neq\alpha}^{N-K} P_{\alpha\to\widetilde{\alpha}}(\xi) = \sum_{q=1}^{N-K} \frac{C(N-K,q)(-1)^{q+1}}{q+1} e^{\frac{-q\rho(\xi)P_{h(\alpha)}}{q+1}} \tag{25}$$

where $P_{h(\alpha)} = |H(\alpha)|^2$ represents the channel gain on subcarrier α.

By applying the Moment Generating Function (MGF) approach to average over the fading channel statistics provided in (25) and using the upper bound of the instantaneous index error probability from (23), the average index error rate $\overline{P}_I(\xi)$ can be derived as follows

$$\overline{P}_I(\xi) \leq \sum_{q=1}^{N-K} K \frac{C(N-K,q)(-1)^{q+1}}{q+1+q\rho(\xi)}. \tag{26}$$

Based on [25], the IBER under CFO distortion can be approximated as

$$P_1(\xi) \approx \frac{\eta}{2}\overline{P}_I(\xi) \tag{27}$$

where $\eta = 1$ for $N > 2$, and $\eta = 2$ for $N = 2$. By substituting (26) into (27), the upper bound of IBER under CFO distortion formula can be expressed as

$$P_1(\xi) \leq \frac{\eta K}{2} \sum_{q=1}^{N-K} \frac{C(N-K,q)(-1)^{q+1}}{q+1+q\rho(\xi)}. \tag{28}$$

This index error probability analysis provides a rigorous quantification of the effect of CFO distortion on index detection errors in OFDM-IM. As evident from the upper bound expression derived, the index error rate under CFO $P_1(\xi)$ has an explicit dependence on the SNR degradation factor $\rho(\xi)$ induced by frequency offset. Therefore, the CFO impairment directly affects the reliability of index detection through interference and SNR loss, which subsequently translates to increased index bit errors in the system.

4.2. Symbol bit errors under CFO

In addition to impacting index bit errors, CFO distortion also degrades the symbol modulation bit error performance in OFDM-IM systems through two mechanisms:

1. Index errors: Inaccurate detection of active subcarrier indices due to CFO distortion results in symbol demodulation on wrong subcarriers, increasing errors.
2. Loss of orthogonality: CFO destroys subcarrier orthogonality, causing ICI that acts as additional noise during coherent symbol detection.

To analyze the joint impact of these factors, we consider two cases:

Case 1. Index correctly detected: If the active index α is accurately detected, the post-detection SNR on subcarrier α gets impacted by ICI under CFO distortion ξ. Let the corresponding symbol error probability be denoted by $P_{M|\alpha}(\xi)$. Using classical modulation analysis, $P_{M|\alpha}(\xi)$ can be derived in terms of the ICI-distorted SNR.

Case 2. Index incorrectly detected: When index α is misdetected as $\tilde{\alpha}$, the receiver loses channel state information for coherent demodulation on subcarrier α. Under moderate-to-high SNR conditions, the symbol error probability in this case can be approximated as 0.5 using non-coherent detection principles. Using total probability theorem, the upper bound of the instantaneous symbol error rate is

$$P_s(\xi) \leq \frac{1}{N}\sum_{\alpha=1}^{N}\left[P_{I|\alpha}(\xi)\cdot 0.5 + \left(1-P_{I|\alpha}(\xi)\right)\cdot P_{M|\alpha}(\xi)\right]. \tag{29}$$

This models the joint impact of index errors and ICI on symbol demodulation under CFO. Substituting the index error probability expression from (23) into (29) by using the fact that $1 - P_{I|\alpha}(\xi) \leq 1$ to get

$$P_s(\xi) \leq \frac{P_I(\xi)}{2K} + \frac{1}{N}\sum_{\alpha=1}^{N} P_{M|\alpha}(\xi). \tag{30}$$

We take the expectation over the index error probability $P_I(\xi)$ and symbol error probability $P_{M|\alpha}(\xi)$ to obtain the SBER as

$$P_2(\xi) \leq \frac{\overline{P}_I(\xi)}{2K} + \overline{P}_M(\xi) \tag{31}$$

where $\overline{P}_M(\xi)$ represents the average symbol error probability. Assuming M-ary phase shift keying (M-PSK) constellation mapping in the AWGN channel, the expression for $\overline{P}_M(\xi)$ can be written as

$$\overline{P}_M(\xi/\phi) = \frac{2}{\max(\log_2 M, 2)} \sum_{i=1}^{\max(1,M/4)} Q\left(\sqrt{2\rho(\xi)\phi}\sin\left(\frac{(2i-1)\pi}{M}\right)\right) \tag{32}$$

where $Q(x) = \frac{1}{\sqrt{2\pi}}\int_x^\infty e^{-y^2/2}\,dy$. Given that $|H_m[k]|$ follows Rayleigh distribution with an average power of P_h, the magnitude squared $|H_m[k]|^2$ follows a chi-square probability density function (PDF) with two degrees of freedom. Consequently, the variable ϕ is also chi-square distributed with two degrees of freedom. To average the expression for M-ary PSK in an additive white Gaussian noise (AWGN) channel over the chi-square distributed random variable ϕ, we have

$$\overline{P}_M(\xi) = \int_0^\infty f(\phi)\overline{P}_M(\xi/\phi)\,d\phi \tag{33}$$

where $f(\phi)$ is the PDF of ϕ. The corresponding SBER expressions in Rayleigh fading channel, as given in [27,28], can be expressed as

$$\overline{P}_M(\xi) \approx \frac{1}{\max(\log_2 M, 2)} \sum_{i=1}^{\max(1,M/4)} (1 - \frac{1}{2}\beta_i(\xi)(3-\beta_i^2(\xi))) \tag{34}$$

where $\beta_i(\xi) = \sqrt{\frac{\rho(\xi)\sin^2\left((2i-1)\frac{\pi}{M}\right)}{1+\rho(\xi)\sin^2\left((2i-1)\frac{\pi}{M}\right)}}$.

Substituting the expressions for $\overline{P}_I(\xi)$ from (26) and $\overline{P}_M(\xi)$ from (34) into (31) yields the following explicit bound:

$$\begin{aligned} P_2(\xi) \quad &\leq \frac{1}{2}\sum_{q=1}^{N-K} \frac{C(N-K,q)(-1)^{q+1}}{q+1+q\rho(\xi)} \\ &+ \frac{1}{\max(\log_2 M, 2)} \sum_{i=1}^{\max(1,M/4)} (1 - \frac{1}{2}\beta_i(\xi)(3-\beta_i^2(\xi))) \end{aligned} \tag{35}$$

The derived upper bound on the symbol error rate $P_2(\xi)$ in (35) demonstrates an explicit dependence on the index error probability $\overline{P}_I(\xi)$. As evident from (26), $\overline{P}_I(\xi)$ is directly affected by the CFO distortion through the SNR degradation factor $\rho(\xi)$. This reveals the inherent coupling between reliability of index detection and accuracy of symbol demodulation in determining overall bit errors under frequency offsets. By substituting the derived upper bound expressions for $P_1(\xi)$ and $P_2(\xi)$ into the total BER formula in (22), the overall performance can be evaluated numerically for given CFO levels. This mathematical analysis reveals how the total bit errors are influenced by the cascading effects of CFO on index detection errors and subsequent faulty symbol demodulation. It provides a means to predict and optimize BER performance under frequency offsets in OFDM-IM systems.

5. Simulation results

The analytical expressions derived in the preceding sections are validated through comprehensive Monte Carlo simulations, providing valuable insights into the performance of OFDM-IM systems under the impact of CFO. The simulations were conducted for various system configurations, involving different subblock sizes N, numbers of active subcarriers K, CFO values ξ, and initial SNR $\rho(0) = \frac{NP_h\sigma_S^2}{K\sigma_b^2}$.

5.1. Simulation setup

The simulations were performed in MATLAB R2022a on a system with an Intel Core i7 processor and 16 GB RAM. QPSK modulation was used, and the channel coefficients were generated according to a frequency-selective Rayleigh fading model, with the channel taps modeled as i.i.d. complex Gaussian random variables with zero mean and unit variance. The CFO values were swept from −0.5 to 0.5, while the SNR range considered was 0 to 50 dB. A total of 10^6 Monte Carlo iterations were performed for averaging the results.

5.2. SNR degradation analysis

Fig. 1 presents a comparative analysis of the impact of CFO on the SNR degradation in the OFDM-IM and classical OFDM systems. The plot depicts the SNR degradation $D(\xi)$ as a function of the initial SNR $\rho(0)$, considering various CFO percentages of 1%, 3%, 6%, and 10% for the OFDM-IM system. The dashed curves represent the SNR degradation for classical OFDM, serving as a reference for comparison. The SNR degradation is calculated using the analytical expression derived in (21) for $N = 4$ and $K = 2$. At lower initial SNR values below approximately 15 dB, the SNR degradation curves for OFDM-IM closely resemble those of classical OFDM, indicating a similar susceptibility to CFO-induced SNR degradation in this regime. However, as the initial SNR increases beyond 15 dB, a notable divergence emerges between the two systems. The OFDM-IM system exhibits a more significant SNR degradation compared to classical OFDM, with the discrepancy becoming increasingly pronounced as the CFO percentage increases. This observation highlights the heightened sensitivity of OFDM-IM to CFO at higher SNR levels and larger CFO values. For instance, at an initial SNR of 30 dB and a CFO of 10%, the OFDM-IM system experiences an SNR degradation of approximately 18 dB, whereas classical OFDM only suffers a degradation of around 15 dB. This confirms the analytical prediction of higher sensitivity to CFO in OFDM-IM arising from disruption of index detection.

Fig. 2 illustrates the relationship between SNR degradation D and CFO ξ at various initial SNRs $\rho(0) = 7, 14$ and 21 dB. It is evident that degradation worsens as frequency offset increases, across all SNRs. Critically, CFO impact is more pronounced at higher nominal SNRs. At 21 dB, the degradation exceeds 5 dB by just $\xi = 0.05$, whereas at 7 dB this threshold is not crossed until $\xi = 0.15$. This reveals CFO's outsized impact specifically in low-medium $\rho(0)$ regimes. Appropriate compensation is therefore critical to maintain SNR performance in these scenarios, where even small offsets can induce substantial degradation. On the other hand, tighter compensation is imperative at higher $\rho(0)$ to achieve robustness against CFO. OFDM-IM always stays more severe degradation than classical OFDM.

The SNR degradation is also influenced by the sparsity ratio (K/N), as shown in Fig. 3. The figure shows the variation in SNR degradation against the sparsity ratio (K/N) for different CFO values. Increased sparsity ratio leads to higher degradation due to a rise in index detection errors. However, the effect is more pronounced at higher CFO. At 10% CFO, the degradation triples from 3 dB to 9 dB as sparsity increases from 0.2 to 0.9. This demonstrates that sparser signal patterns require tighter CFO control. The analysis provides a means to determine suitable sparsity ratios based on CFO limits to constrain performance loss. This impairment effect is less formal in OFDM-IM as the IM bits carried over sparse subcarriers suffer from CFO distortion.

5.3. Index BER (IBER) performance

Fig. 4 illustrates the severe detrimental impact of CFO on IBER performance in the OFDM-IM system. The plot depicts both theoretical curves and simulation results for IBER versus initial SNR under different CFO percentages ranging from 0% to 10%. While CFO increases IBER throughout the SNR range, the most dramatic worsening is observed

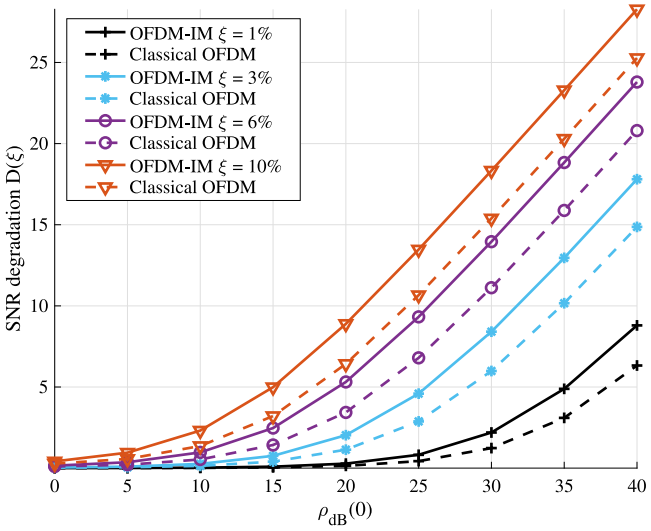

Fig. 1. SNR degradation $D(\xi)$ Vs. initial SNR $\rho(0)$ for different CFO values.

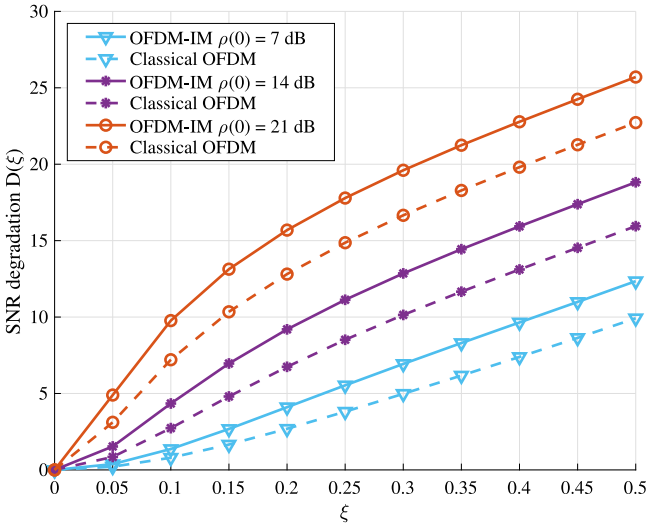

Fig. 2. SNR degradation $D(\xi)$ Vs. CFO for different initial SNRs values.

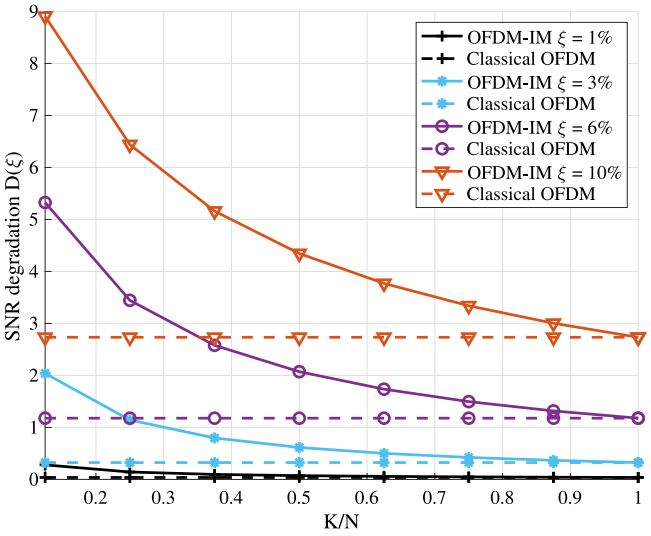

Fig. 3. SNR degradation $D(\xi)$ Vs. CFO for different Sparsity Ratio (K/N) values.

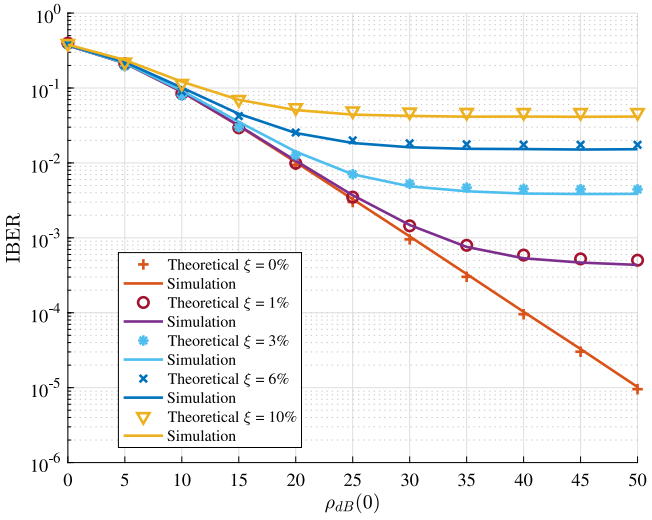

Fig. 4. IBER Vs. initial SNR $\rho(0)$ for different CFO values.

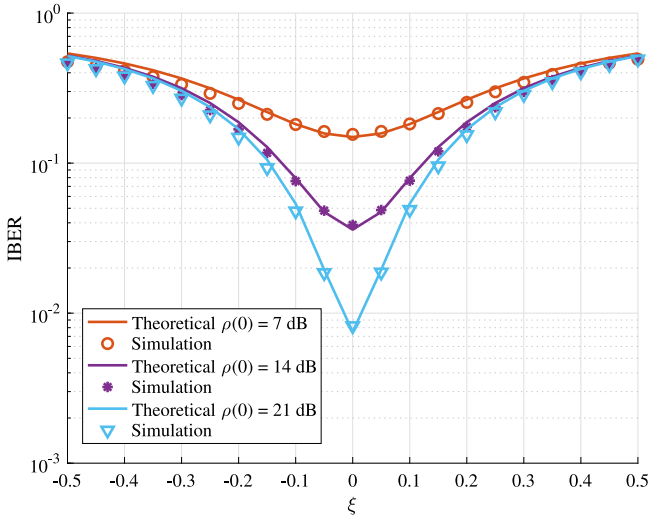

Fig. 5. IBER Vs. CFO for different initial SNRs values.

at higher SNRs above 15 dB. In this regime, even minor CFO values result in a considerable increase in IBER by several orders of magnitude compared to the ideal case of 0% CFO. This extreme sensitivity to small offsets at higher SNRs highlights the critical need for strict CFO compensation techniques to maintain reliable index detection and low IBER performance. By quantifying the relationship between IBER, SNR, and CFO, Fig. 4 provides critical insights for system design. Robust CFO mitigation techniques are imperative to constrain the IBER penalty, particularly in low-to-medium SNR environments where the effects are most crippling. Minor offsets can severely reduce index detection accuracy. This analysis shows that IM in CFO-impaired channels relies significantly on strict compensation to achieve potential improvements. The simulated IBER values closely match the theoretical curves, validating the theoretical analysis.

The variation of IBER with respect to CFO values for different SNR levels is illustrated in Fig. 5. the figure shows the IBER performance over a CFO range of −0.5 to 0.5 for three different initial SNR values: $\rho(0) = 7, 14$ and 21 dB. IBER worsens symmetrically with increasing CFO magnitude due to disrupted index detection,with more precipitous degradation observed at lower SNRs. To quantify the impact, maintaining a target IBER of 10^{-3} requires CFO to be constrained within ±0.1 at 7 dB SNR, ±0.25 at 14 dB, and ±0.4 at 21 dB. This decrease in CFO tolerance at higher SNRs demonstrates that compensation requirements are dependent on SNR; at higher SNRs, stricter thresholds are required to limit IBER, whereas at lower SNRs, where the impact is diminished, more laxity exists.

5.4. BER performance

Fig. 6 presents the influence of CFO on the BER performance in the OFDM-IM system. The plot exhibits theoretical curves and simulation results illustrating BER versus SNR across varying CFO percentages from 0% to 10%. Similar to Fig. 4's depiction of IBER, CFO detrimentally affects BER performance across all SNR levels. The degradation in BER due to CFO follows a comparable trend to that observed for IBER, with the impact being particularly pronounced at higher SNRs. The simulated BER values closely match the theoretical curves, validating the analytical models used to quantify the relationship between BER, SNR, and CFO in the OFDM-IM system. This consistency reinforces the importance of robust CFO compensation techniques to ensure reliable communication performance in OFDM-IM systems.

While the SNR levels presented in Fig. 6 may appear high, it is important to note that these results are for uncoded systems. Channel coding techniques, such as the turbo codes discussed in [29], could potentially allow for operation at lower SNR levels while maintaining acceptable performance. However, the analysis of coded systems is beyond the scope of this paper, which focuses on isolating the fundamental impact of CFO on OFDM-IM.

Fig. 7 plots the BER against a CFO range of −0.5 to 0.5 for multiple initial SNR levels, illustrating the increased susceptibility of BER to CFO as SNR decreases. It shows that CFO not only affects IBER accuracy but also significantly impacts overall bit error performance, especially in challenging SNR environments. This reinforces the need for adaptive CFO compensation strategies that take into account the operating SNR level to optimize system performance.

To quantify the cascading impact of SNR degradation on BER, Fig. 8 plots the BER against the SNR degradation factor $D(\xi)$ induced by CFO in the OFDM-IM system at initial SNR values of 7 dB, 14 dB, and 21 dB. Increased degradation leads to a sharp rise in BER, particularly at lower SNR values. For instance, at an initial SNR of 7 dB, the BER surges above the critical threshold of 10^{-1} for all SNR degradation values shown, indicating a severe performance breakdown even with modest CFO values. However, at a higher 21 dB SNR, the BER remains below 10^{-1} even for degradations up to 15 dB. This quantifies the cascading effect of CFO-induced SNR loss on the final BER performance. The study shows a link between the desired BER and the worst possible SNR loss, which can help determine how much CFO compensation is needed to keep distortion effects to a minimum. Overall, the results support the analytical framework for measuring how CFO, SNR degradation, and BER affect each other in order to improve system reliability.

6. Conclusions

This paper has presented a comprehensive analytical framework to quantify the performance degradation effects of CFO on OFDM-IM systems operating over frequency-selective fading channels. Novel closed-form expressions are derived for the CFO-induced SNR degradation and tight upper bound for the BER performance. The analysis accounted for both IM errors and distortion in data symbol demodulation due to CFO. Extensive simulations validate the accuracy of the analytical models and provide insights into mitigating CFO impacts through effective system parameter selection and compensation techniques. The findings yield valuable insights into mitigating CFO-induced degradation in OFDM-IM through effective compensation techniques and optimized system parameter selection. This work contributes significantly towards realizing reliable and spectrally efficient OFDM-IM communication

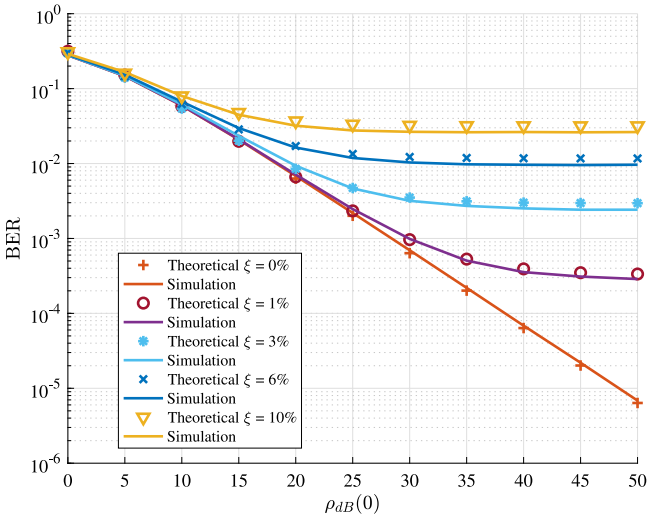

Fig. 6. BER Vs. initial SNR $\rho(0)$ for different CFO values.

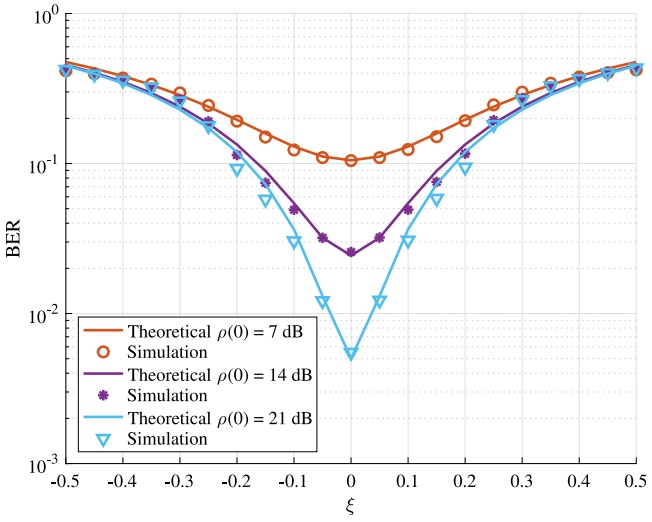

Fig. 7. BER Vs. CFO for different initial SNRs values.

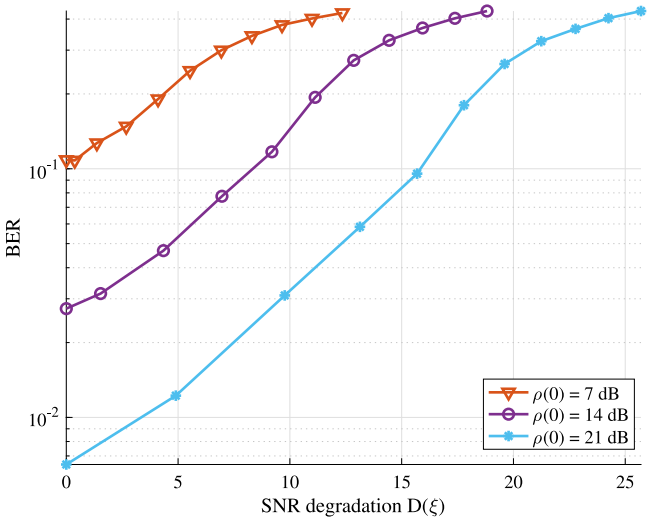

Fig. 8. BER Vs. SNR degradation $D(\xi)$ for different initial SNRs values.

links that are resilient to carrier frequency offsets and dispersive channel conditions. Future research can focus on creating more advanced CFO estimation and compensation algorithms that work well with OFDM-IM, taking advantage of its unique features like embedded pilot patterns and sparsity.

CRediT authorship contribution statement

Mokhtar Besseghier: Writing – review & editing, Writing – original draft, Visualization, Validation, Supervision, Software, Project administration, Methodology, Formal analysis, Conceptualization. **Samir Ghouali:** Writing – review & editing, Software, Methodology, Investigation. **Ahmed Bouzidi Djebbar:** Writing – review & editing, Supervision, Resources, Formal analysis. **Ertugrul Basar:** Writing – review & editing, Validation, Supervision, Project administration, Formal analysis.

Declaration of competing interest

The authors declare that they have no known competing financial interests or personal relationships that could have appeared to influence the work reported in this paper.

Data availability

No data was used for the research described in the article.

References

[1] R. Du, S. Wang, F. Liu, Broad learning system-based detector for OFDM with index modulation, IEEE Commun. Lett. 27 (1) (2023) 224–228, http://dx.doi.org/10.1109/LCOMM.2022.3216304.

[2] E. Basar, U. Aygolu, E. Panayırcı, H.V. Poor, Orthogonal frequency division multiplexing with index modulation, IEEE Trans. Signal Process. 61 (22) (2013) 5536–5549, http://dx.doi.org/10.1109/TSP.2013.2279771.

[3] S. Dogan Tusha, A. Tusha, E. Basar, H. Arslan, Multidimensional index modulation for 5G and beyond wireless networks, Proc. IEEE 109 (2) (2021) 170–199.

[4] M. Besseghier, S. Ghouali, A.B. Djebbar, Optimized greedy detection for OFDM-IM systems, IEEE Commun. Lett. 27 (8) (2023) 2034–2037, http://dx.doi.org/10.1109/LCOMM.2023.3283032.

[5] Z. Xie, W. Yi, X. Wu, Y. Liu, A. Nallanathan, Exploiting index modulation for enhanced NOMA, in: GLOBECOM 2023 - 2023 IEEE Global Communications Conference, 2023, pp. 4915–4920, http://dx.doi.org/10.1109/GLOBECOM54140.2023.10437466.

[6] W. Jin, M. Wang, G. Yang, Z. Chen, Energy-efficient and fading-resistant multi-mode OFDM-IM with high dimensional mapping, IEEE Trans. Wirel. Commun. (2022) 1, http://dx.doi.org/10.1109/TWC.2022.3230461.

[7] M. Wen, E. Basar, Q. Li, B. Zheng, M. Zhang, Multiple-mode orthogonal frequency division multiplexing with index modulation, IEEE Trans. Commun. 65 (9) (2017) 3892–3906, http://dx.doi.org/10.1109/TCOMM.2017.2710312.

[8] J. Li, S. Dang, Y. Huang, P. Chen, X. Qi, M. Wen, H. Arslan, Composite multiple-mode orthogonal frequency division multiplexing with index modulation, IEEE Trans. Wireless Commun. 22 (6) (2023) 3748–3761, http://dx.doi.org/10.1109/TWC.2022.3220752.

[9] M. Wen, J. Li, S. Dang, Q. Li, S. Mumtaz, H. Arslan, Joint-mapping orthogonal frequency division multiplexing with subcarrier number modulation, IEEE Trans. Commun. 69 (7) (2021) 4306–4318, http://dx.doi.org/10.1109/TCOMM.2021.3066584.

[10] J. Li, S. Dang, M. Wen, Q. Li, Y. Chen, Y. Huang, W. Shang, Index modulation multiple access for 6G communications: Principles, applications, and challenges, IEEE Netw. 37 (1) (2023) 52–60, http://dx.doi.org/10.1109/MNET.002.2200433.

[11] M. Wen, Q. Li, K.J. Kim, D. López-Pérez, O.A. Dobre, H.V. Poor, P. Popovski, T.A. Tsiftsis, Private 5G networks: Concepts, architectures, and research landscape, IEEE J. Sel. Top. Sign. Proces. 16 (1) (2022) 7–25, http://dx.doi.org/10.1109/JSTSP.2021.3137669.

[12] M. Wen, S. Lin, K.J. Kim, F. Ji, Cyclic delay diversity with index modulation for green internet of things, IEEE Trans. Green Commun. Netw. 5 (2) (2021) 600–610, http://dx.doi.org/10.1109/TGCN.2021.3067705.

[13] Z. Yang, F. Chen, B. Zheng, M. Wen, W. Yu, Carrier frequency offset estimation for OFDM with generalized index modulation systems using inactive data tones, IEEE Commun. Lett. 22 (11) (2018) 2302–2305, http://dx.doi.org/10.1109/LCOMM.2018.2869772.

[14] J. Lee, H.-L. Lou, D. Toumpakaris, J. Cioffi, Effect of carrier frequency offset on OFDM systems for multipath fading channels, in: IEEE Global Telecommunications Conference, 2004, Vol. 6, GLOBECOM '04, 2004, pp. 3721–3725 Vol.6, http://dx.doi.org/10.1109/GLOCOM.2004.1379064.
[15] L. Khalid, A. Anpalagan, Effect of carrier frequency offset on the BER performance of variable spreading factor OFCDM systems, in: 2008 IEEE Int. Conf. Commun., 2008, pp. 5038–5042, http://dx.doi.org/10.1109/ICC.2008.945.
[16] L.F. Xie, I.W.-H. Ho, Z. Situ, P. Li, The impact of CFO on OFDM based physical-layer network coding with QPSK modulation, in: 2020 IEEE Wireless Communications and Networking Conference, WCNC, 2020, pp. 1–6, http://dx.doi.org/10.1109/WCNC45663.2020.9120461.
[17] Q. Ma, P. Yang, Y. Xiao, H. Bai, S. Li, Error probability analysis of OFDM-IM with carrier frequency offset, IEEE Commun. Lett. 20 (12) (2016) 2434–2437, http://dx.doi.org/10.1109/LCOMM.2016.2600646.
[18] B. Satwika, K. Hari, An analysis for the performance of the OFDM-IM systems impaired by carrier frequency offset, in: 2021 29th European Signal Processing Conference, EUSIPCO, 2021, pp. 1661–1665, http://dx.doi.org/10.23919/EUSIPCO54536.2021.9616135.
[19] Y. Ko, A tight upper bound on bit error rate of joint OFDM and multi-carrier index keying, IEEE Commun. Lett. 18 (10) (2014) 1763–1766, http://dx.doi.org/10.1109/LCOMM.2014.2347280.
[20] I. Erol Gurol, E. Basar, D. Kucukyavuz, F. Atay Onat, A novel orthogonal frequency division multiplexing with index modulation waveform with carrier frequency offset resistance and low peak-to-average power ratio, Int. J. Commun. Syst. 35 (7) (2022) e5094, http://dx.doi.org/10.1002/dac.5094.
[21] J. Liu, M. Wang, X. Feng, Synchronization algorithm of 5G new waveform based on index modulation, in: 2022 IEEE 95th Veh. Technol. Conf.: (VTC2022-Spring), 2022, pp. 1–6, http://dx.doi.org/10.1109/VTC2022-Spring54318.2022.9860842.
[22] E. Basar, Index modulation techniques for 5G wireless networks, IEEE Commun. Mag. 54 (7) (2016) 168–175, http://dx.doi.org/10.1109/MCOM.2016.7509396.
[23] D. Zhang, K. Niu, Polar-coded OFDM with index modulation, IEEE Trans. Veh. Technol. 73 (4) (2024) 5335–5347, http://dx.doi.org/10.1109/TVT.2023.3332775.
[24] T.T.H. Le, X.N. Tran, V.-D. Ngo, M.-T. Le, Repeated index modulation-OFDM with coordinate interleaving: performance optimization and low-complexity detectors, IEEE Syst. J. 15 (3) (2021) 3673–3681, http://dx.doi.org/10.1109/JSYST.2020.3029072.
[25] J. Crawford, E. Chatziantoniou, Y. Ko, On the SEP analysis of OFDM index modulation with hybrid low complexity greedy detection and diversity reception, IEEE Trans. Veh. Technol. 66 (9) (2017) 8103–8118, http://dx.doi.org/10.1109/TVT.2017.2691778.
[26] T. Van Luong, Y. Ko, Impact of CSI uncertainty on MCIK-OFDM: tight closed-form symbol error probability analysis, IEEE Trans. Veh. Technol. 67 (2) (2018) 1272–1279, http://dx.doi.org/10.1109/TVT.2017.2753402.
[27] M. Besseghier, A.B. Djebbar, A. Zouggaret, I. Dayoub, Joint channel estimation and data detection for OFDM based cooperative system, Telecommun. Syst. 73 (4) (2020) 545–556, http://dx.doi.org/10.1007/s11235-019-00622-3.
[28] K. Cho, D. Yoon, On the general BER expression of one- and two-dimensional amplitude modulations, IEEE Trans. Commun. 50 (7) (2002) 1074–1080, http://dx.doi.org/10.1109/TCOMM.2002.800818.
[29] K. Vasudevan, Coherent detection of turbo-coded OFDM signals transmitted through frequency selective Rayleigh fading channels with receiver diversity and increased throughput, Wirel. Pers. Commun. 82 (3) (2015) 1623–1642, http://dx.doi.org/10.1007/s11277-015-2303-8.

Dr. Mokhtar Besseghier was born in 1987 in Mascara, Algeria. He received the Master's degree in Telecommunications from MASCARA University in 2012 and the Ph.D. degree from Sidi Bel Abbes University, Algeria, in 2017. He is currently an Associate Professor at the University of Mascara in the department of Electronics, and he does his research at the Telecommunication and Digital Signal Processing Laboratory at Sidi Bel Abbes University. His current research interests are in wireless communications and digital signal processing.

Dr. Samir Ghouali received his Master's degree in Mobile Networks and Services from the University of Tlemcen (Algeria) in 2012. Currently, he serves as an MCA researcher at the Faculty of Sciences and Technology, Mustapha Stambouli University of Mascara, Algeria. His research interests revolve around the development of telemedicine applications on smartphones for monitoring individuals in high-risk situations. He also holds a strong interest in mobile networks and services.

Dr. Ahmed bouzidi Djebbar was born in 1972. He received State Engineering degree, Master degree and Ph.D. degree with honor from electronic department of Sidi Bel Abbes University in 1995, 1999 and 2006 respectively. He joined Sidi Bel Abbes University as assistant professor in 2000. From 2005 to 2006, he was scholarship at OAE Department of Valenciennes University, France and at the Signal and Image Processing Department of ENST, Paris, France. His-research interest are in adaptive low complexity Blind and Semi-Blind algorithms for MIMO multicarrier systems, performance analysis and multiuser detection.

Prof. Ertugrul Basar was born in 1985 in Istanbul, is an Associate Professor at Koç University's Electrical and Electronics Engineering Department and Director of its Communications Research Lab. He earned his B.S. from Istanbul University (2007), and M.Sc. (2009) and Ph.D. (2013) from Istanbul Technical University, where he previously worked as a faculty member.

His research focuses on beyond 5G/6G wireless, MIMO, reconfigurable surfaces, waveform design, physical layer security, and signal processing/deep learning for communications. He has 10 patents and over 160 journal publications with 14,000+ citations.

Prof. Basar has received numerous awards, including the IEEE ComSoc Best Young Researcher Award (2020) and was elevated to IEEE Fellow in 2023 for his contributions to next-gen wireless physical layer design. He has supervised 22 graduate students and serves on editorial boards of several journals.